

Superfluid Transition Temperature in a Fermi Gas with Repulsion. Higher Orders Perturbation Theory Corrections.

D.V. Efremov^{a1}, M.S. Mar'enko^{a2}, M.A. Baranov^b, M.Yu. Kagan^a

^a *P.L. Kapitza Institute for Physical Problems, Moscow 117334, Russia*

^b *Russian Research Center "Kurchatov Institute", Moscow 123182, Russia*

October 29, 2018

Abstract

High order perturbation theory corrections to the superfluid transition temperature in a weakly interacting Fermi gas with repulsive interaction are calculated. This involves calculating the contributions of third and fourth order diagrams in the gas parameter ap_F and taking into account effects of retardation. The contributions from both second, third and fourth orders result in the effective attraction in p -wave channel. It is shown that the critical temperature is mainly determined by second and third orders terms of perturbation theory. The dependence of the critical temperature on an external magnetic field is found. We discuss possible applications of the results to the diluted ^3He - ^4He mixtures and trapped neutral-atom Fermi gases.

PACS: 67.60.-g, 74.20.-z, 74.20.Mn

1 Introduction

Unconventional mechanisms of Cooper pairing have recently started to attract greater attention. This is primarily related to the discovery of high-temperature superconducting (HTSC) systems, superconductivity in organic materials and heavy-fermion compounds, and also because of the search for superfluidity in of ^3He - ^4He mixtures and in trapped atomic Fermi gases. However, HTSC and heavy-fermion systems belong to a class of strongly correlated systems whose theoretical analysis requires the development of new methods. At the same time, ^3He - ^4He mixtures and trapped atomic Fermi gases can be described using the model of a weakly interacting Fermi gas. In this case the interparticle

¹E-mail:efremov@kapitza.ras.ru

²E-mail:maxim@kapitza.ras.ru

interaction can be either attractive or repulsive. In the attractive case conventional singlet Cooper pairing takes place where the orbital momentum of the pair is $\ell = 0$, for which the critical temperature was first calculated by Gor'kov and Melik-Barkhudarov [1]. In systems with repulsive interaction, the formation of $\ell = 0$ Cooper pairs is clearly impossible and in order to investigate the existence of superfluidity, we need to study the possibility of $\ell \neq 0$ Cooper pairing. The possible existence of superfluidity in Fermi systems with repulsion was first indicated by Kohn and Luttinger in 1965. In [2] they examined the contribution of collective effects to the scattering amplitude in a particle-particle channel which lead to effective quasiparticle interaction at the Fermi surface via polarization of the Fermionic background. A principal role in the formation of attractive harmonics in the effective interaction and consequently the superfluidity is played by the Kohn singularity in the effective interaction. In the three-dimensional case, it has the form

$$\tilde{\Gamma}_{\text{eff}}^{\text{sing}}(q) \sim \left[(2p_F)^2 - q^2 \right] \ln \left| (2p_F)^2 - q^2 \right| + \Gamma_{\text{reg}}(q^2). \quad (1)$$

In coordinate space the Kohn singularity leads to alternating sign and magnitude dependent RKKY-type interaction between quasiparticles:

$$\tilde{\Gamma}_{\text{eff}}^{\text{sing}}(r) \sim \frac{1}{r^3} \cos(2p_F r + \varphi).$$

It should be noted that the above contribution to the effective interaction decreases over large distances more slowly than the bare interaction $U_0(r - r')$ and consequently corresponds to the main contribution to the scattering amplitude in the limit of large momenta ℓ [2]:

$$\tilde{\Gamma}_{\text{eff}}^{(\ell)} \sim \frac{(-1)^\ell}{l^4}.$$

A simple extrapolation made by the authors of [2] yields extremely low estimates for superfluid transition temperatures in the limit $l \rightarrow 2$: 10^{-16} and 10^{-11} for ${}^3\text{He}$ and the electron subsystem in the metal, respectively. It was subsequently shown in [3], [4] that effective attraction occurs also for the angular momentum $\ell = 1$ which gives the following expression for the critical triplet-pairing temperature in the second order of perturbation theory:

$$T_{c1} \sim \tilde{\varepsilon} \exp \left\{ -\frac{5\pi^2}{4(2 \ln 2 - 1)(ap_F)^2} \right\} \approx \tilde{\varepsilon} \exp \left\{ -\frac{13.0}{\lambda^2} \right\}. \quad (2)$$

where $\lambda = (2ap_F)/\pi$ is the gas parameter, a is the s -wave scattering length, p_F is the Fermi momentum, and $\tilde{\varepsilon}$ is the energy parameter, of the order of the Fermi energy, which provides a cutoff at high energies. Substituting experimental values for ${}^3\text{He}$ where triplet pairing takes place, gives good agreement with experiment: $T_{c1} \sim 10^{-3}\text{K}$. (Obviously, the bare interaction in real ${}^3\text{He}$ is far more complex than that in the considered model). The aim of the present paper is to determine the critical superfluid transition temperature of a weakly non-ideal Fermi gas with repulsive interparticle interaction up to the preexponential factor. For this purpose we calculate the irreducible vertex in the Cooper channel in the third and fourth orders of perturbation theory with respect to the gas parameter λ . We

also allow for renormalization of the singular parts of the Green's functions (corrections associated with the Z -factor and the effective mass) in the Bethe-Salpeter equation (3) and take into account retardation effects (the influence of the frequency and momentum dependencies of the irreducible vertex). This article is organized as follows. In Section 2 we derive and analyze an equation for the critical temperature in a weakly interacting Fermi gas with repulsion. In Section 3 we calculate the irreducible vertex in the Cooper channel in the second, third, and fourth orders of perturbation theory. In Section 4 we examine the contribution of retardation effects. In Sections 5 and 6 we give the final formula for the critical temperature and discuss the contribution of the bare scattering in the p -wave channel. In Section 7 we note the possibility of a strong enhancement of T_{c1} in an external magnetic field. In Section 8 we discuss possible experimental applications of the obtained results. In particular, we discuss the possibility of triplet Cooper pairing in ^3He - ^4He mixtures and in a trapped neutral-atom Fermi gases at ultralow temperatures.

2 Superfluid transition in a Fermi gas with repulsion

We consider a weakly interacting Fermi gas described by the Hamiltonian

$$\begin{aligned} \hat{H} &= \hat{H}_0 + \hat{H}_{\text{int}} = \sum_{\alpha \mathbf{p}} (\varepsilon_{\mathbf{p}} - \mu) \hat{a}_{\mathbf{p}\alpha}^\dagger \hat{a}_{\mathbf{p}\alpha} + \\ &+ \frac{g}{2} \sum_{\alpha\beta \mathbf{p}\mathbf{p}'\mathbf{q}} \hat{a}_{\mathbf{p}\alpha}^\dagger \hat{a}_{\mathbf{p}'\beta}^\dagger \hat{a}_{\mathbf{p}'+\mathbf{q}\beta} \hat{a}_{\mathbf{p}-\mathbf{q}\alpha}, \end{aligned}$$

where the indices $\alpha, \beta = 1, 2$ label the system components which we assume to have equal masses m and concentrations $n_{1,2} = p_F^3/6\pi^2$, μ is the chemical potential, and the constant g characterizes the interparticle interaction which we shall assume to be point-like (here and subsequently we put $\hbar = 1$). The specific physical meaning of the two components depends on the particular system. For example, for ^3He - ^4He mixtures it corresponds to an "upward" and "downward" projection of the spin, whereas in the case of trapped atomic gas, it corresponds to a hyperfine-structure component (or projection of the nuclear spin). The considered form of the interparticle interaction assumes that only s -wave scattering takes place in the system, characterized by the scattering length a . (In the leading order of perturbation theory $a = mg/4\pi$.) The corresponding small dimensionless parameter, the gas parameter λ , is given by $\lambda = 2|a|p_F/\pi$. We subsequently show how the final result is modified in the presence of scattering in channels with nonzero orbital momenta. It is well known that the appearance of superfluid pairing is associated with the presence of a pole in the two-particle vertex function Γ in the particle-particle channel (Cooper channel) for zero total momentum and frequency [5]. This vertex function Γ is a solution of the Bethe-Salpeter integral equation (Fig. 1):

$$\begin{aligned} \Gamma(p_1, -p_1; p_3, -p_3) &= \tilde{\Gamma}(p_1, -p_1; p_3, -p_3) - \\ -T \sum_{n=-\infty}^{+\infty} \int \tilde{\Gamma}(p_1, -p_1; q, -q) G(\omega_n, \mathbf{q}) G(-\omega_n, -\mathbf{q}) \Gamma(q, -q; p_3, -p_3) \frac{d^3q}{(2\pi)^3}, \end{aligned} \quad (3)$$

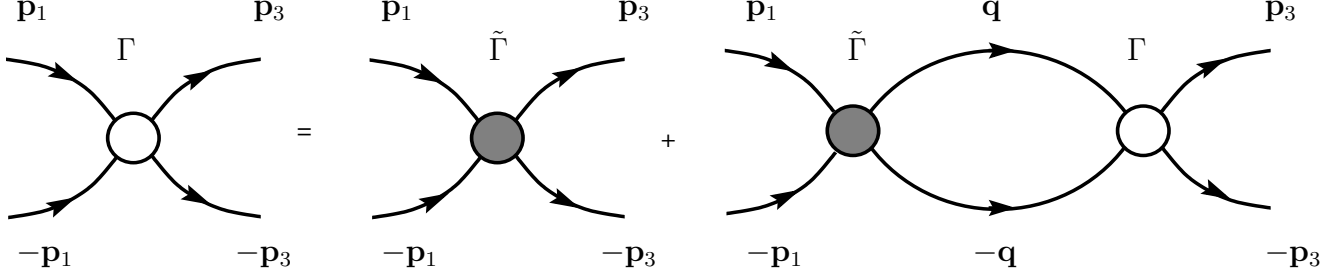


Figure 1: Bethe-Salpeter equation for complete vertex Γ .

where $\tilde{\Gamma}$ is the irreducible vertex in the Cooper channel (having no singularities at zero total momentum and frequency), G is the single-particle Green's function, and the arguments of the vertex functions denote the corresponding sets of Matsubara frequencies and momenta: $q = (\omega_n, \mathbf{q})$, $p_1 = (\omega_{n1}, \mathbf{p}_1)$, and so on. Note that in formula (3) (and in the following formulas) we do not explicitly indicate the indices distinguishing the components of the Fermi gas (for example, Γ should be considered as $\Gamma_{\alpha\beta\gamma\delta}$, and so on). Writing them in explicit form does not present any difficulties. We also note that the nonsymmetrized (in terms of the component indices) irreducible vertex function is used in equation (3). The vertex functions Γ and $\tilde{\Gamma}$ appearing in (3) are in fact functions of the Matsubara frequencies, the absolute values of the incoming and outgoing momenta, and the angle between them. For example, we have

$$\Gamma(p_1, -p_1; p_3, -p_3) = \Gamma(\omega_1, \omega_3, |\mathbf{p}_1|, |\mathbf{p}_3|, \cos(\theta_{\mathbf{p}_1\mathbf{p}_3})).$$

Thus, expanding G and as a series in terms of Legendre polynomials

$$\begin{aligned} \tilde{\Gamma}(\dots, \cos(\theta)) &= \sum_{l=0}^{+\infty} (2l+1) \tilde{\Gamma}_l(\dots) P_l(\cos \theta), \\ \Gamma(\dots, \cos(\theta)) &= \sum_{l=0}^{+\infty} (2l+1) \Gamma_l(\dots) P_l(\cos \theta) \end{aligned} \quad (4)$$

and integrating over angles, we easily obtain from (3) the following equation for the singular part $\Gamma_l^{(s)}$ of the l -th harmonic of the vertex function:

$$\Gamma_l^{(s)}(\omega_1, \omega_3, |\mathbf{p}_1|, |\mathbf{p}_3|) = \quad (5)$$

$$-T \sum_{n=-\infty}^{+\infty} \int \frac{d^3q}{(2\pi)^3} \tilde{\Gamma}_l(\omega_1, \omega_n, |\mathbf{p}_1|, |\mathbf{q}|) G(\omega_n, \mathbf{q}) G(-\omega_n, -\mathbf{q}) \Gamma_l^{(s)}(\omega_n, \omega_3, |\mathbf{q}|, |\mathbf{p}_3|).$$

As usual, the critical temperature corresponds to the appearance of a nontrivial solution of this equation which is related to singular (logarithmic) behavior of the Cooper loop near the Fermi surface. Thus, in order to determine the critical temperature in the leading order in λ , it is sufficient to set the frequencies to zero and the absolute values of the momenta to p_F in all the vertex functions contained in (5). We then have

$$-T \sum_n \int \frac{d^3q}{(2\pi)^3} G(\omega_n, q) G(-\omega_n, -q) \rightarrow \frac{m^*}{m} Z^2 \nu_F \ln \frac{\tilde{\varepsilon}}{T_{c1}}, \quad (6)$$

where $\nu_F = mp_F/2\pi^2$ is the density of states at the Fermi surface, m^* is the effective mass, and Z is the residue in the singular part of the single-particle Green's function. In equation (6) $\tilde{\varepsilon} \sim \varepsilon_F$ is the cutoff parameter which depends on the behavior of $\tilde{\Gamma}$ at high momenta and frequencies. Now equation (5) can be rewritten in the form

$$\Gamma_l^{(s)} = \tilde{\Gamma}_l \cdot Z^2 \frac{m^*}{m} \nu_F \ln \left(\frac{\tilde{\varepsilon}}{T} \right) \cdot \Gamma_l^{(s)}, \quad (7)$$

where $\tilde{\Gamma}_l = \tilde{\Gamma}_l(p_i = p_F, \omega_i = 0)$ $\Gamma_l^{(s)} = \Gamma_l^{(s)}(p_i = p_F, \omega_i = 0)$, so that a nontrivial solution is only possible for $\tilde{\Gamma} < 0$ and occurs at temperature $T = T_{cl}$ where

$$T_{cl} = \tilde{\varepsilon} \exp \left\{ -\frac{1}{\nu_F |\tilde{\Gamma}_l|} \frac{m}{m^* Z^2} \right\}. \quad (8)$$

For the case of a Fermi gas with interparticle attraction we have $\tilde{\Gamma}_0 \simeq 4\pi a/m < 0$, and the system is unstable with respect to traditional s -wave pairing ($\ell = 0$). The superfluid transition temperature in this case was obtained in [1] to within terms $O(\lambda^0)$ and is given by

$$T_{c0} = \frac{1}{\pi} e^C \left(\frac{2}{e} \right)^{7/3} \varepsilon_F \exp \left\{ -\frac{\pi}{2|a|p_F} \right\} \approx 0.28 \varepsilon_F \exp \left\{ -\frac{1}{\lambda} \right\}, \quad (9)$$

where $C = 0.58 \dots$ is the Euler constant. This expression only differs from the corresponding expression for T_{c0} in BCS theory in that the Debye frequency ω_D is replaced by ε_F in the preexponential factor. This replacement means that in our case the entire Fermi sphere and not only its vicinity of the order of the Debye frequency, is involved in the pairing. Note that in order to find the preexponential factor in [1] we need to calculate $\tilde{\Gamma}_0$ to within terms of the second order of perturbation theory.

For repulsive interaction, $a > 0$, equation (5) for $\ell = 0$ only has a trivial solution and s -wave pairing is impossible. In this case, superfluid pairing will take place in the channel having the orbital momentum ℓ for which $\tilde{\Gamma}_l$ is negative and has the maximum absolute value. As it is well known [6], the scattering amplitude of slow particles with the orbital momentum ℓ for the short-range potential has the order of magnitude $a(ap)^{2\ell}$, where p is the particle momentum and a is the s -wave scattering length. Thus, in our particular case

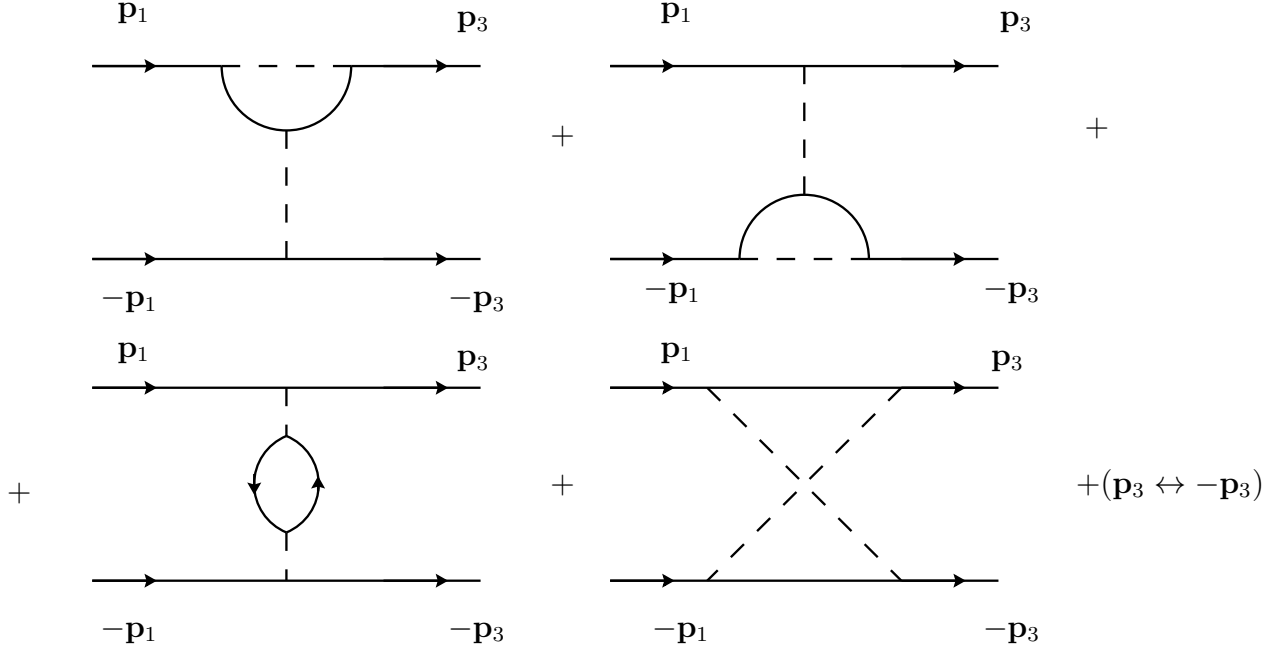


Figure 2: Second-order diagrams in terms of gas parameter for irreducible interaction.

the corresponding contribution to $\tilde{\Gamma}_l$ with $l > 0$ from scattering on the bare interparticle potential has a maximum for $l = 1$ and has the order $(ap_F)^3 \sim \lambda^3$. At the same time, many-particle effects associated with polarization processes of the Fermi background in a Fermi gas have the order λ^2 and, therefore, dominates for $l \geq 1$ [4]. Corresponding diagrams for $\tilde{\Gamma}$ in the second order with respect to λ are plotted in Fig. 2. For our particular case of point interaction the first three diagrams cancel out so that $\tilde{\Gamma}$ is completely determined by the last exchange diagram and is given by (we assumed $T = 0$)

$$\tilde{\Gamma}(\omega_1, \omega_3, \mathbf{p}_1, \mathbf{p}_3) = \left(\frac{4\pi a}{m}\right)^2 \Pi(\omega_1 + \omega_3, \mathbf{p}_1 + \mathbf{p}_3),$$

where

$$\Pi(\Omega, \mathbf{q}) = \int \frac{d\omega}{2\pi} \int \frac{d^3p}{(2\pi)^3} G(\omega, \mathbf{p}) G(\Omega + \omega, \mathbf{p} + \mathbf{q}) = \int \frac{d^3p}{(2\pi)^3} \frac{n(\mathbf{p} + \mathbf{q}) - n(\mathbf{p})}{\Omega + \xi(\mathbf{p} + \mathbf{q}) - \xi(\mathbf{p})}. \quad (10)$$

In this expression $n(p)$ is the Fermi particle distribution function for $T = 0$, $\xi(p) = p^2/2m - \mu$.

From formula (10) we can easily obtain an expression for the irreducible vertex at zero external frequencies and momenta lying on the Fermi surface. In terms of the angle θ

between \mathbf{p}_1 and \mathbf{p}_3 we have

$$\nu_F \tilde{\Gamma}(0, 0, p_1 = p_F, p_3 = p_F, \cos \theta) = \frac{\pi \lambda}{2} \left(1 - \frac{\lambda}{2} \left[1 + \frac{\sqrt{2}(1 + \cos \theta)}{4\sqrt{1 - \cos \theta}} \ln \frac{\sqrt{2} + \sqrt{1 - \cos \theta}}{\sqrt{2} - \sqrt{1 - \cos \theta}} \right] \right).$$

As a result of the integration with Legendre polynomials we obtain

$$\nu_F \tilde{\Gamma}_1 = \frac{1}{5} \lambda^2 (1 - 2 \ln 2) < 0. \quad (11)$$

All the other partial components $\tilde{\Gamma}_\ell$ with $\ell > 1$ also correspond to attraction but are smaller than $\tilde{\Gamma}_1$ and their absolute values decrease rapidly with increasing ℓ (see [4]). Thus, we conclude that a weakly interacting Fermi gas with interparticle repulsion is unstable with respect to triplet p -wave pairing. The corresponding critical temperature in the leading order with respect to λ is

$$T_{c1} = \tilde{\varepsilon} \exp \left\{ -\frac{1}{\nu_F |\tilde{\Gamma}_1|} \right\} = \tilde{\varepsilon} \exp \left\{ -\frac{5}{(2 \ln 2 - 1) \lambda^2} \right\}. \quad (12)$$

It can be seen from this formula that in order to determine the preexponential factor $\tilde{\varepsilon}$ in equation (5) we need to retain terms up to order λ^4 . (This follows from the fact that since $\tilde{\Gamma}_1$ begins from terms λ^2 , to obtain terms of the order λ^0 in the exponent, we need to know $\tilde{\Gamma}_1$ up to terms λ^4 includingly.)

Note that the contribution of triple collisions can be neglected within the considered accuracy since it has the order λ^5 [5, §6].

3 Contribution of higher orders of perturbation theory

The irreducible vertex $\tilde{\Gamma}$ in the third and fourth orders of perturbation theory is given by the diagrams shown in Figs. 3 and 4, respectively. The points on these diagrams correspond to antisymmetrized two-particle interaction. In expanded notation when the interaction is represented as a dashed line (as in Fig. 2) these corresponds to two different ways of connecting the incoming and outgoing lines.

Figures 3 and 4 only give skeleton diagrams (without the self-energy insertions) and Fig. 4 only gives "nonoriented" diagrams. The corresponding Feynman diagrams are obtained by arranging the arrows on the lines (taking into account the particle number conservation at the vertexes) and also the incoming and outgoing momenta. Figure 5 shows an example of such an arrangement.

Direct calculations of these diagrams using standard rules of the diagram technique yield diverging expressions as a result of the integration over large momenta in subdiagrams containing Cooper loops (loops formed from two lines in the same direction). For example, we consider the first third-order diagram in Fig. 3 together with the corresponding diagram

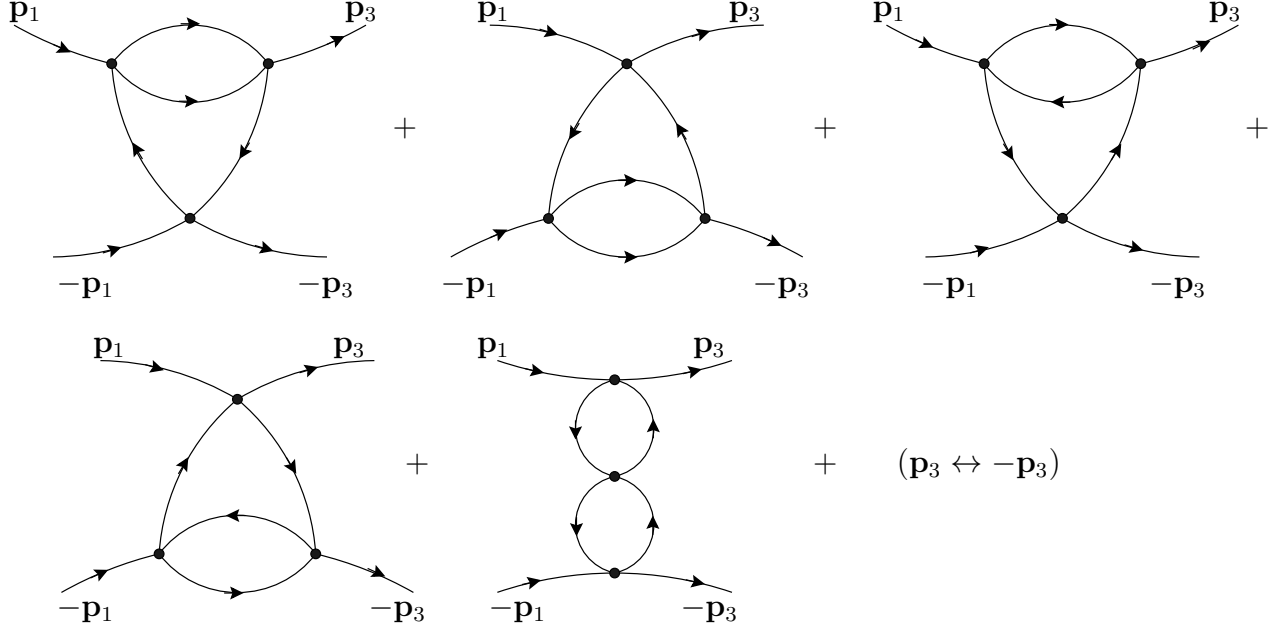


Figure 3: Skeleton diagrams of the third order of perturbation theory for the irreducible vertex $\tilde{\Gamma}$

in which p_3 is replaced with $-p_3$. In expanded form they correspond to the sum of the diagrams in Fig. 6 where the dashed line is the interparticle interaction. It is easily to check that for short-ranged potential the first three diagrams cancel out leaving only the fourth diagram which contains a subdiagram diverging at large momenta, corresponding to a Cooper loop between two parallel dashed lines. However, this subdiagram is the first correction of a ladder series to the one of the dashed lines on the fourth diagram in Fig. 2 which gives a contribution to in the second order with respect to λ . In the same way, the second diagram in Fig. 3 together with the corresponding diagram in which p_3 is replaced with $-p_3$ in the sum is the correction to the second dashed line on the same diagram in Fig. 2.

These corrections only differ from the first term of the Born series for the scattering amplitude in that they contain the single-particle Green's functions in the medium G and not in vacuum $G^{(0)}$. However, at large momenta the difference between G and $G^{(0)}$ disappears so that the divergence in the diagram in Fig. 7 can be eliminated by changing from the bare interaction g to the scattering length a (renormalization procedure). This scattering length a is determined by the scattering amplitude of two particles in vacuum in the limit where the energies of the colliding particles tend to zero and can be obtained from the equation

$$\frac{4\pi a}{m} = g + \int \frac{d\omega}{2\pi} \int \frac{d^3 p}{(2\pi)^3} g G^{(0)}(\omega, p) G^{(0)}(-\omega, -p) \frac{4\pi a}{m} = \quad (13)$$

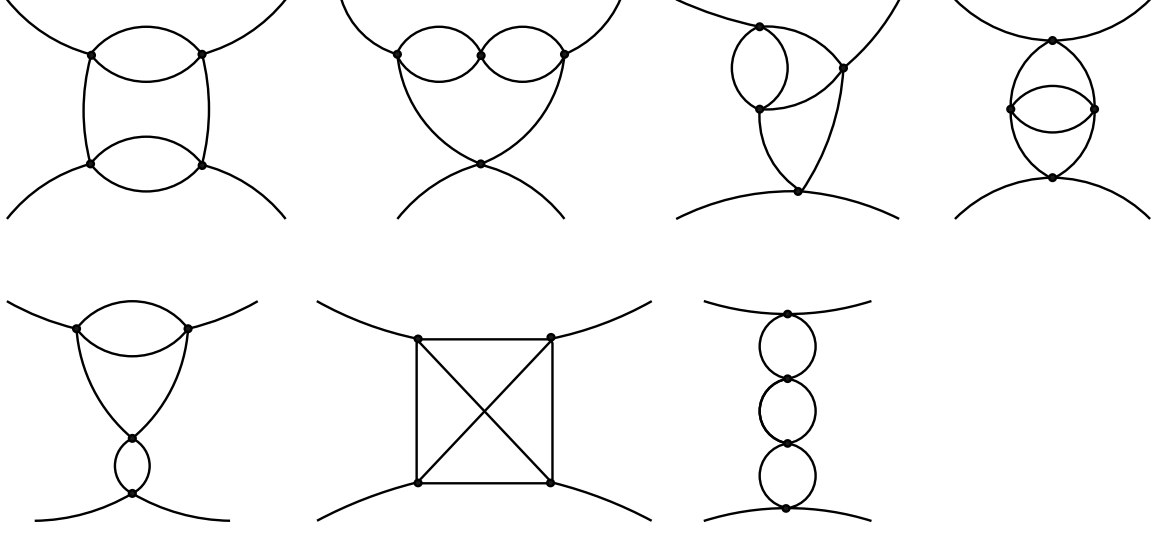


Figure 4: Skeleton "nonoriented" diagrams of the fourth order of perturbation theory for the irreducible vertex $\tilde{\Gamma}$.

$$= g + \int \frac{d^3p}{(2\pi)^3} g \frac{1}{2\varepsilon(p) + i0} \frac{4\pi a}{m}.$$

After integrating in diagram Fig. 6d over the intermediate frequency of the Cooper loop ω , we obtain the expression

$$\int \frac{d^4q}{(2\pi)^4} \int \frac{d^3p}{(2\pi)^3} \left(\frac{1 - \theta(\xi_1) - \theta(\xi_2)}{\Omega - (\xi_1 + \xi_2) + i\delta(\text{sign}\xi_1 + \text{sign}\xi_2)} \right) \times \frac{1}{(\Omega - \xi_3 + i\delta\text{sign}\xi_3)(\Omega - \xi_4 + i\delta\text{sign}\xi_4)}, \quad (14)$$

where $\xi_1 = \xi(\mathbf{p} + \frac{\mathbf{q}+\mathbf{w}}{2})$, $\xi_2 = \xi(-\mathbf{p} + \frac{\mathbf{q}+\mathbf{w}}{2})$, $\xi_3 = \xi(\mathbf{q} - \mathbf{s})$, $\xi_4 = \xi(\mathbf{q} + \mathbf{s})$, $\mathbf{p}_1 = \mathbf{s} + \mathbf{w}$, $\mathbf{p}_3 = \mathbf{s} - \mathbf{w}$. The integral over the internal momentum \mathbf{p} of the expression in brackets diverges at large momentum. As we have already noted, this divergence is of the same type as the Born correction to the scattering amplitude. Therefore, the divergence in the considered third order diagram can be eliminated by replacing the bare interaction constant g with the scattering length a in the second order diagram in Fig. 2d.

To within the required accuracy the relationship between g and a can be obtained from (13) and has the form

$$\begin{aligned} g &= \frac{4\pi}{m} a + \left(\frac{4\pi}{m} a \right)^2 \int \frac{d^3p d\omega}{(2\pi)^4} G^{(0)}(\omega, \mathbf{p}) G^{(0)}(-\omega, -\mathbf{p}) \\ &= \frac{4\pi}{m} a + \left(\frac{4\pi}{m} a \right)^2 \int \frac{d^3p}{(2\pi)^3} \frac{1}{2\varepsilon(p) + i\delta}, \end{aligned} \quad (15)$$

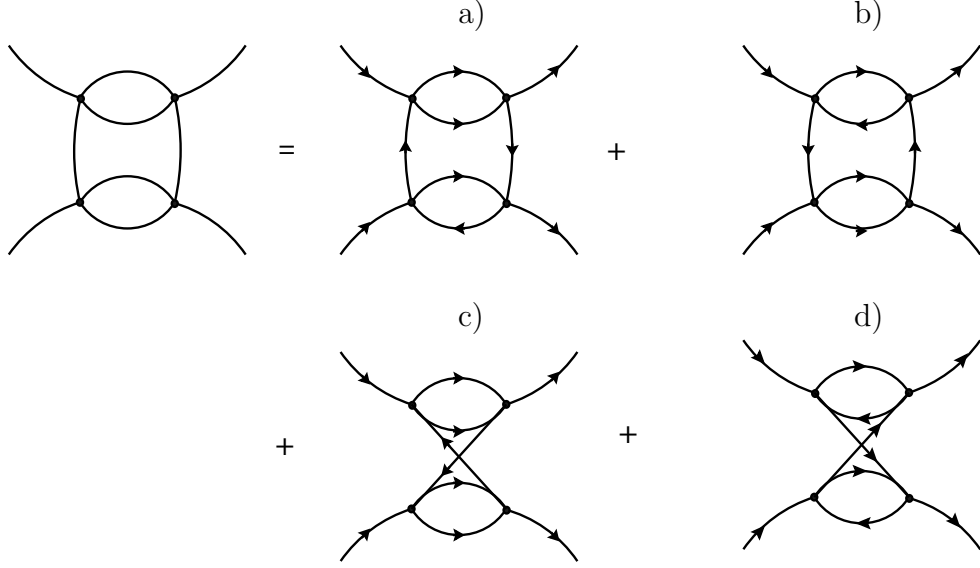


Figure 5: Example of decoding "nonoriented" diagrams (first diagram in Fig. 4).

where $\varepsilon(p) = \frac{p^2}{2m}$. The renormalization procedure is shown schematically as follows:

$$\nu_F \{g^2 \Pi + 2g^3 (GG) \tilde{\Pi}\} \rightarrow \lambda^2 \Pi + 2\lambda^3 [(GG) - (G^{(0)}G^{(0)})] \tilde{\Pi}, \quad (16)$$

where (GG) corresponds to the first cofactor in formula (14), $\tilde{\Pi}$ corresponds to the second cofactor,

$$(G^{(0)}G^{(0)}) = \int \frac{d\omega}{2\pi} G^{(0)}(\omega, -\mathbf{p}) G^{(0)}(\omega, -\mathbf{p}) = \frac{1}{2\varepsilon(p) + i\delta},$$

and the factor 2 in second term in (16) results from the contribution of the second diagram in Fig. 3. As we can easily see, the expression for $\tilde{\Pi}$, being integrated over frequency, gives the polarization operator Π which appears in the first term in formula (16). The last term in formula (16) can be explicitly written as

$$\begin{aligned} \Gamma^{(3a)} &= -2i \left(\frac{2\pi^2 \lambda}{mp_F} \right)^3 \int \frac{d^4 q}{(2\pi)^4} \int \frac{d^3 p}{(2\pi)^3} \frac{1}{(\Omega - \xi_3 + i\delta \text{sign} \xi_3)(\Omega - \xi_4 + i\delta \text{sign} \xi_4)} \quad (17) \\ &\times \left(\frac{1 - \theta(\xi_1) - \theta(\xi_2)}{\Omega - (\xi_1 + \xi_2) + i\delta(\text{sign} \xi_1 + \text{sign} \xi_2)} - \frac{1}{2\varepsilon(p) + i\delta} \right). \end{aligned}$$

This expression contains no divergences and can be integrated numerically. It can be checked that all other third-order diagrams contain no divergences and, as a result of numerical calculations, we obtain the final result for the third-order contribution to the

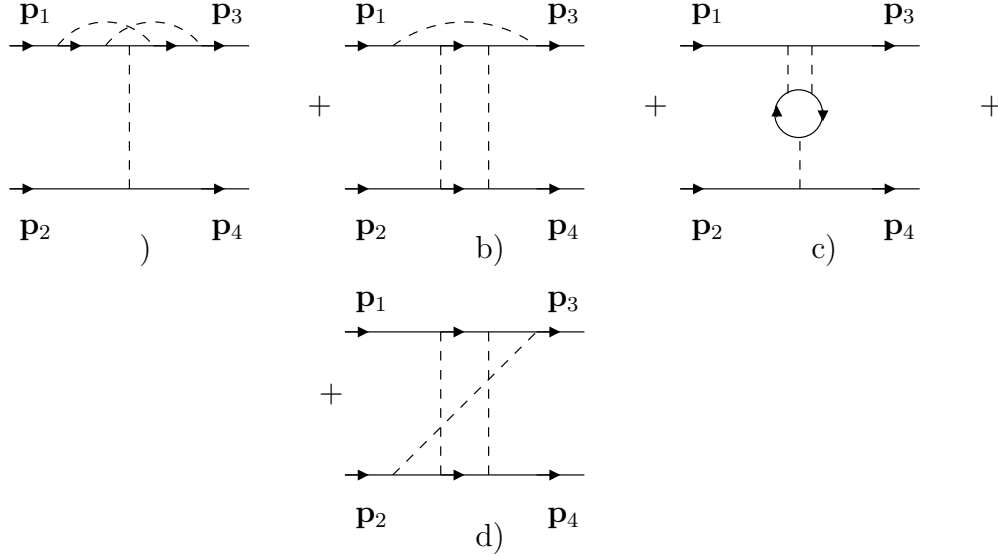


Figure 6: First third-order diagram from Fig. 3 showing diagram corresponding to the substitution $\mathbf{p}_3 \rightarrow -\mathbf{p}_3$, in expanded representation.

p -wave harmonic of the irreducible vertex:

$$\nu_F \tilde{\Gamma}_1^{(3)} = -0.33\lambda^3. \quad (18)$$

It should be noted that formula (18) contains no contribution from Hartree-Fock self-energy components in the second-order diagrams since this contribution corresponds to renormalization of the chemical potential. We also note that the appearance of a large numerical coefficient 0.33 (compared with the coefficient of 0.077 for the second-order contribution) is associated with the stronger angular dependence of the third-order diagrams (see Fig. 8). This dependence is mainly determined by the first two diagrams in Fig. 3 and can be attributed to the existence of subdiagrams with Cooper loops.

All divergences in the fourth-order diagrams can be eliminated in exactly the same way. For this purpose, in the third-order diagrams we need to express g in terms of a in accordance with formula (15) and in the second-order diagrams, express g in terms of a allowing for the term $\sim a^3$, which can easily be obtained from equation (13). (This term is required to eliminate the divergences in the second diagram in Fig. 4.) As a result, the contribution of the fourth-order diagrams in Fig. 4 is given by

$$\nu_F \tilde{\Gamma}_1^{(4)} = -0.39\lambda^4. \quad (19)$$

In order to calculate $\tilde{\Gamma}_1$ to within λ^4 we also need to allow for the contribution of the self-energy insertions of the second order in λ in the second-order diagrams $\tilde{\Gamma}_1^{(2)}$, see Fig. 2. These contributions can no longer be reduced to renormalization of the chemical potential.

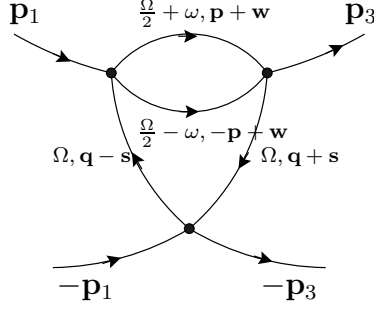


Figure 7: Diagram of the third order of perturbation theory containing a Cooper loop as subdiagram.

They also result in the appearance of a non-trivial Z -factor and the effective mass m^* [7]:

$$Z = 1 - \lambda^2 \ln 2; \quad \frac{m^*}{m} = 1 + \frac{2}{15}(7 \ln 2 - 1)\lambda^2 \quad (20)$$

in the singular part of the single-particle Green's function which now also contains a regular part proportional to λ^2 . By means of direct numerical calculations of the corresponding diagrams we can establish that the contribution of the latter to $\tilde{\Gamma}_1$ is negligible. Thus, we finally obtain the following expression with the required accuracy in terms of λ for the irreducible vertex in a Cooper channel with orbital momentum $\ell = 1$:

$$\begin{aligned} \nu_F Z^2 \frac{m^*}{m} \tilde{\Gamma}_1 &= \nu_F Z^2 \frac{m^*}{m} \left(Z^2 \frac{m^*}{m} \tilde{\Gamma}_1^{(2)} + \tilde{\Gamma}_1^{(3)} + \tilde{\Gamma}_1^{(4)} \right) \\ &= -0.077\lambda^2 - 0.33\lambda^3 - 0.26\lambda^4. \end{aligned} \quad (21)$$

4 The retardation effects

In order to determine the critical temperature in Section 2, in equation (5) we replaced the irreducible vertex $\tilde{\Gamma}_1$, which is a function of the incoming and outgoing frequencies and absolute values of momenta $\tilde{\Gamma}_1(\omega_i, \mathbf{p}_i)$, by its value at zero frequencies and momenta lying on the Fermi surface $\tilde{\Gamma}_1(\omega_i = 0, \mathbf{p}_i = p_F)$. In this section we shall show that allowance for the difference between $\tilde{\Gamma}_1(\omega_i, \mathbf{p}_i)$ and $\tilde{\Gamma}_1(\omega_i = 0, \mathbf{p}_i = p_F)$ (retardation effects) introduces a correction of the order of λ^4 to the vertex $\tilde{\Gamma}_1$. In other words, these effects influence the numerical coefficient in the preexponential factor.

Retardation effects are most conveniently taken into account using a method proposed in [8, . 2]. Omitting the appropriate procedures, which are a trivial generalization of the derivation of [8] to the case of p -wave pairing, we arrive at the following integral equation:

$$\Phi_1(\xi) = - \int_{-\varepsilon_F}^{\infty} d\xi' \frac{\text{th } \xi'/2T}{2\xi'} R_1(\xi, \xi') \Phi_1(\xi'), \quad (22)$$

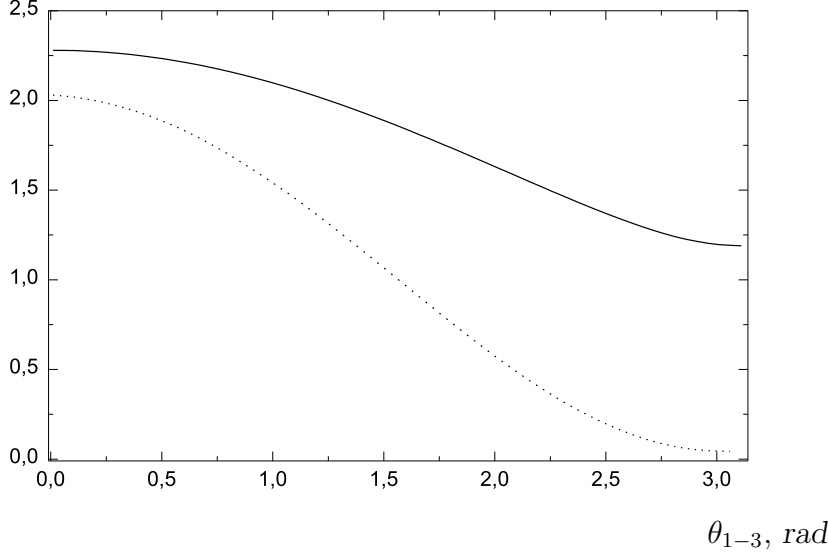


Figure 8: Dependence of the irreducible vertex in the second and third orders on the angle between the incoming and outgoing momenta θ_{1-3} : $\Gamma^{(2)}/\lambda^2$ – solid curve, $\Gamma^{(3)}/\lambda^3$ – dashed curve.

for which the condition for existence of a nontrivial solution determines the critical temperature T_{c1} . The unknown function Φ_1 in (22) can be related to the spectral density of the anomalous Green's function (or more accurately to its first harmonic in the expansion in terms of Legendre polynomials), and the kernel $R_1(\xi, \xi')$ is given by

$$R_1(\xi, \xi') = \frac{m}{4\pi^2 p^2(\xi)} \int_{|p(\xi) - p(\xi')|}^{p(\xi) + p(\xi')} q dq \int_0^\infty \frac{dE \sigma(E, m)}{E + |\xi| + |\xi'|} \frac{p^2(\xi) + k^2(\xi') - q^2}{2k(\xi')}, \quad (23)$$

where $\sigma(E, q)$ is related to $\tilde{\Gamma}(\omega = \omega_1 - \omega_3, \mathbf{q} = \mathbf{p}_1 - \mathbf{p}_3)$ by

$$\tilde{\Gamma}(i\omega_n, \mathbf{p}) = \int_0^\infty \frac{dE^2 \sigma(E, \mathbf{p})}{E^2 + \omega_n^2}, \quad (24)$$

and the factor $(p^2 + k^2 - q^2)/2pk$ is precisely the cosine of the angle between the incoming and outgoing momenta which picks up the first harmonic in the expansion (4) in terms of Legendre polynomials.

Dividing the region of integration over ξ' in equation (22) into three parts: $|\xi'| \leq z\varepsilon_F$, $-\varepsilon_F < \xi' < -z\varepsilon_F$, and $\xi' > z\varepsilon_F$, where z is an arbitrary number satisfying the condition $T_{c1} \ll z\varepsilon_F \ll \varepsilon_F$, and integrating by parts (where the dependence on ξ' in $R(\xi, \xi')$ and $\Phi_1(\xi')$ can be neglected in the first region and the hyperbolic tangent in the second and

third regions can be replaced by ∓ 1 , respectively), equation (22) can be reduced to the form

$$\Phi_1(\xi) = -\ln\left(\frac{2\gamma\varepsilon_F}{\pi T_{c1}}\right)\Phi_1(0)R_1(\xi, 0) + \frac{1}{2}\int_{-\varepsilon_F}^{\infty} d\xi' \ln\left(\frac{|\xi'|}{\varepsilon_F}\right) \frac{d}{d\xi'} (R_1(\xi, \xi')\Phi_1(\xi')). \quad (25)$$

(As was to be expected, the arbitrary constant z was dropped from this equation.) We introduce the new variable

$$\chi(\xi) = \frac{\Phi_1(\xi)}{\Phi_1(0) \ln \frac{\pi T_{c1}}{2\gamma\varepsilon_F}}, \quad (26)$$

which allows us to write the expression for the critical temperature in the form

$$T_{c1} = \frac{2e^C}{\pi}\varepsilon_F \exp\left(-\frac{1}{\chi(0)}\right), \quad (27)$$

where the function $\chi(\xi)$ satisfies

$$\chi(\xi) = R_1(\xi, 0) + \frac{1}{2}\int_{-\varepsilon_F}^{\infty} d\xi' \ln\left(\frac{|\xi'|}{\varepsilon_F}\right) \frac{d}{d\xi'} (R_1(\xi, \xi')\chi(\xi')) \quad (28)$$

Since the kernel R_1 contains the small parameter ($R \sim \lambda^2$), equation (22) can be solved by an iterative method. In the zeroth approximation we set:

$$\chi^{(0)}(\xi) = R_1(\xi, 0).$$

The first correction $\chi^{(1)}$ is given by the integral on the right-hand side of (28) with $\chi = \chi^{(0)}$:

$$\chi^{(1)} = \frac{1}{2}\int_{-\varepsilon_F}^{\infty} d\xi' \ln\left(\frac{|\xi'|}{\varepsilon_F}\right) \frac{d}{d\xi'} (R_1(\xi, \xi')R_1(\xi', 0)) \quad (29)$$

and, as can easily be seen, begins with terms of the order λ^4 . The leading term with respect to λ in χ_1 is obtained if only the leading ($\sim \lambda^2$) terms are retained in the kernel R_1 in formula (29). In this case, the spectral function $\sigma(E, \mathbf{q})$ is the same as the imaginary part of the operator

$$\begin{aligned} \sigma(E, \mathbf{q}) &= -\frac{1}{\pi}\text{Im}\Pi(E, \mathbf{q}) = \\ &= -\frac{1}{\pi} \begin{cases} -\frac{mp_F}{4\pi\tilde{q}} \left[1 - \left(\frac{\tilde{E}}{\tilde{q}} - \frac{\tilde{q}}{2} \right)^2 \right] & \text{at } \left| \frac{\tilde{q}^2}{2} - \tilde{q} \right| \leq \tilde{E} \leq \frac{\tilde{q}^2}{2} + \tilde{q} \\ -\frac{mp_F}{4\pi\tilde{q}} 2\tilde{E} & \text{at } 0 \leq \tilde{E} \leq \tilde{q} - \frac{\tilde{q}^2}{2}, \end{cases} \end{aligned}$$

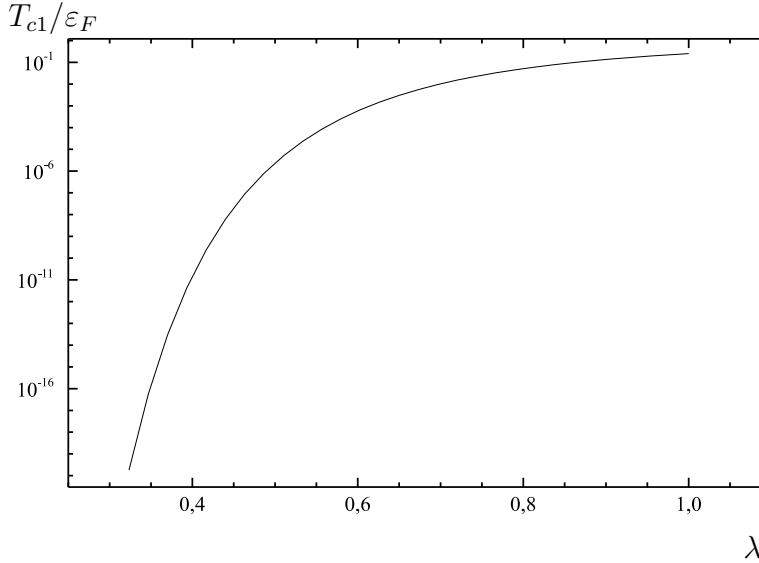


Figure 9: Dependence of T_{c1}/ϵ_F on the gas parameter λ .

where $\tilde{q} = q/p_F$, $\tilde{E} = Em/p_F^2$. Direct calculations using formula (29) give $\chi^{(1)} \approx 0.004\lambda^4$ which is equivalent to adding $\Delta\tilde{\Gamma}_1$ in formula (8),

$$\nu_F \Delta\tilde{\Gamma}_1 \approx 0.004\lambda^4. \quad (30)$$

Note that a similar estimate of the contributions of retardation effects was made in [9] where the authors used the step function approximation for the frequency dependence of the polarization operator.

5 Critical temperature T_{c1}

Collecting above results together [formulas (21) and (30)], we obtain the following expression for the critical temperature which is determined numerically to within two decimal places:

$$T_{c1} = \frac{2}{\pi} e^C \epsilon_F \exp \left\{ -(0.077\lambda^2 + 0.33\lambda^3 + 0.26\lambda^4)^{-1} \right\} \longrightarrow \xrightarrow{\lambda \rightarrow 0} \frac{2}{\pi} e^C \epsilon_F \exp \left\{ -\frac{13.0}{\lambda^2} + \frac{42.0}{\lambda} - 190 \right\}, \quad (31)$$

where the omitted terms have the order λ . This last formula assumes $\lambda < 0.23$ since for $\lambda = 0.23$ the second- and third-order terms with respect to λ in the exponential function in (31) are the same. For $0.23 \leq \lambda \leq 1$ the fourth-order term with respect to λ in (31) is smaller than the first two so that (31) can accurately be rewritten in the form

$$T_{c1} \approx \frac{2}{\pi} e^C \epsilon_F \exp \left\{ -\frac{13.0}{\lambda^2(1 + 4.3\lambda)} + \frac{42.0}{(1 + 4.3\lambda)^2} \right\} \quad (32)$$

This formula may be considered as an extrapolation of the expression for the critical temperature from $\lambda \ll 1$ [formula (31)] to the region $\lambda < 1$ [formula (32)]. The dependence $T_{c1}(\lambda)$ is shown in Fig. 9.

6 Influence of bare p -wave scattering

So far we have only considered s -wave scattering between particles, assuming that the interparticle potential is a point-like. However, as we have already pointed out, for the potential with a finite range, the problem will always contain scattering having an arbitrary orbital momentum ℓ whose amplitude for particles having momenta equal to the Fermi momentum p_F may be estimated as $f_\ell \sim a(ap_F)^{2\ell}$ [6]. From this it follows that with the required accuracy we can confine our analysis to p -wave scattering ($\ell = 1$). In this case, only two contributions will be important: a contribution of the order λ^3 from p -wave scattering at the bare interparticle potential and a contribution of the order λ^4 corresponding to the diagram in Fig. 2d where one of the dashed lines corresponds to s -wave scattering and the other to p -wave scattering. More precisely, if the amplitude of p -wave scattering of two particles having momenta p_F is written in the form

$$f_1 = \alpha_1 a \left(\frac{2ap_F}{\pi} \right)^2 = \alpha_1 a \lambda^2, \quad (33)$$

α_1 is a numerical coefficient of order unity, the contribution of triplet scattering to the irreducible vertex $\tilde{\Gamma}_1$ has the form

$$\nu_F \tilde{\Gamma}_1 = \alpha_1 \lambda^3 (1 + 0.008\lambda).$$

We can see that the fourth-order contribution with respect to λ can be neglected and consequently the critical temperature is given by

$$T_{c1} = \frac{2}{\pi} e^C \varepsilon_F \exp \left\{ -\frac{13.0}{\lambda^2 [1 + (4.3 + \alpha_1)\lambda]} + \frac{42.0}{[1 + (4.3 + \alpha_1)\lambda]^2} \right\}. \quad (34)$$

Nevertheless, we can specify a physical situation when the contribution of p -wave scattering can be neglected. This corresponds to the case when a shallow level having the orbital momentum $\ell = 0$ (resonance scattering) exists in the potential. In this case, the p -wave scattering amplitude is estimated as $f_1 \sim r_0(r_0 p_F)^2$, where r_0 is the radius of action of the potential while the s -wave scattering length is given by $a = (1/2m|E|)^{1/2} \gg r_0$, where E is the discrete level energy (we assume that the condition $|E| \gg \varepsilon_F$ is satisfied so that $ap_F \ll 1$). Then for α_1 in formula (34) we obtain the estimate

$$\alpha_1 \sim \left(\frac{r_0}{a} \right)^3 \ll 1,$$

and if the condition

$$\alpha_1 \ll \lambda$$

is satisfied, the contribution of the p -wave harmonic of the bare interparticle interaction can be neglected compared with the fourth order of the effective interaction which allows only for s -wave scattering.

7 Critical temperature in a magnetic field

In this section we study the influence of an external magnetic field on the irreducible vertex $\tilde{\Gamma}_1$ and consequently on the critical temperature T_{c1} to within terms of the order λ^3 . As was shown in [10], in the leading approximation with respect to λ in the model being studied the critical p -wave pairing temperature may increase appreciably if a static magnetic field is applied to the system. This is because for conventional singlet pairing the role of a magnetic field is always destructive due to the paramagnetic suppression of Cooper pairing caused by the flipping of one of the pair spins. However for triplet p -wave pairing no paramagnetic effect occurs so that the role of the magnetic field is not clear a priori.

In our approach the mechanism for variation of T_{c1} in a magnetic field is based on the magnetic field dependence of the many-particle effects which determine the effective interaction. On the one hand, as a result of a difference in the number of particles (and consequently Fermi momenta) with spins directed parallel and antiparallel to the field, the Kohn singularity increases sharply, causing an increase in $\tilde{\Gamma}_1$. On the other hand, $\nu_{F\downarrow}\tilde{\Gamma}_1$ value decreases with increasing magnetic field because of a monotonic decrease in the number of particles with spin antiparallel to the field. (We recall that s -wave scattering can only occur between Fermi particles having different spin projections.) Competition between these two effects leads to a sharply non-monotonic dependence of the critical temperature on the magnetic field (more accurately, on the degree of polarization $\alpha = (n_\uparrow - n_\downarrow)/(n_\uparrow + n_\downarrow)$) with pronounced increase in T_{c1} for small α , a maximum at intermediate α , and a decrease for $\alpha \rightarrow 1$. (In this case of a completely polarized Fermi gas only p -wave scattering between parallel spins can only take place.) The dependence of $\tilde{\Gamma}$ on the polarization α to within second-order terms was calculated in [10]:

$$\tilde{\Gamma}^{(2)}(\delta) = -\lambda^2 \frac{2 \ln 2 - 1}{5} \frac{1}{\delta^3} \left(\frac{2}{1 + \delta^3} \right)^{2/3} \left[1 + \frac{\delta - 1}{3(2 \ln 2 - 1)} \Psi_\delta \right], \quad (35)$$

where

$$\Psi_\delta = (\delta + 1) \left[10 \ln(\delta + 1) - \delta^2 - 3 \right] + \frac{\delta - 1}{2} (\delta^3 + 2\delta^2 + 8\delta + 4) \ln \frac{\delta + 1}{\delta - 1} + \frac{6}{\delta - 1} \ln \frac{(\delta + 1)}{2},$$

$$\delta = \frac{p_{F\uparrow}}{p_{F\downarrow}} = \left(\frac{1 + \alpha}{1 - \alpha} \right)^{1/3}.$$

In the third order with respect to λ the result can only be obtained numerically. The corresponding contribution is given by the diagrams in Fig. 3 where the spins on the outer lines are directed parallel to the field and those in the inner loops can be oriented either parallel or antiparallel to the field. The calculations (including renormalization of the diverging diagrams) are exactly the same as in the absence of a magnetic field and the result is shown in Fig. 10 (solid curve) which also contains the second-order contribution (35) for comparison (dashed curve).

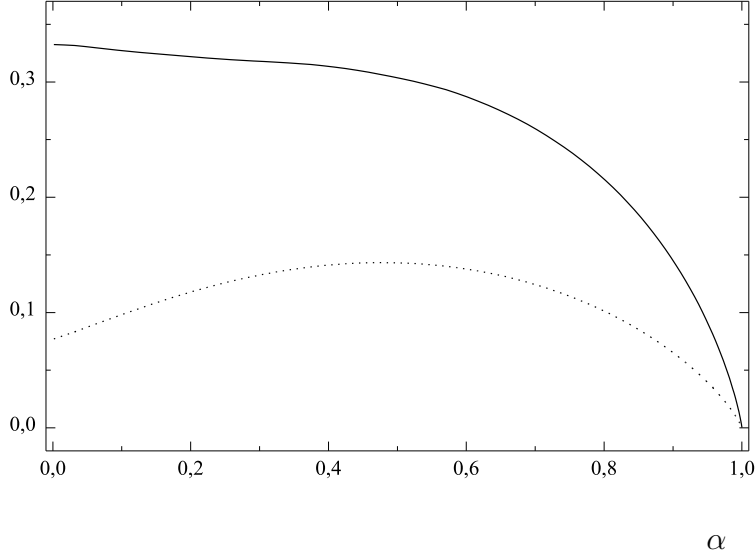


Figure 10: Dependence of the second- and third-order contributions to the irreducible vertex on the degree of polarization α : $\Gamma^{(2)}/\lambda^2$ – dashed curve, $\Gamma^{(3)}/\lambda^3$ – solid curve.

It can be seen that the maximum of $\tilde{\Gamma}_1^{(2)}(\alpha)$ is obtained at $\alpha_m = 0.48$ whereas $\tilde{\Gamma}_1^{(3)}(\alpha)$ decreases monotonically. Thus, the maximum of T_{c1} is determined by competition between increasing $\tilde{\Gamma}_1^{(2)}(\alpha)$ and decreasing $\tilde{\Gamma}_1^{(3)}(\alpha)$. For typical λ this is in the region of $\alpha \sim 0.4$. Graphs of the critical temperature as a function of the degree of polarization are shown in Fig. 11 for typical values of λ . For $\lambda = 0.6$ the value of T_{c1} at the maximum is approximately six times large than the value of T_{c1} in the absence of the field. In the latter case the maximum is mainly determined by the second order and is reached at $\lambda \sim 0.45$.

8 Discussion of the results

The experimental search for nontrivial pairing with $l \neq q1$ in isotropic Fermi systems has recently been actively pursued. Until recently the main candidate was ${}^3\text{He}$ - ${}^4\text{He}$ mixture. So far superfluidity has not yet been observed in this system although temperatures of the order of $97 \mu\text{K}$ have been achieved experimentally [11]. In the concentration range $x < x_0 \approx 3\%$ the scattering length in the mixture correspond to the attraction so that singlet s -wave pairing may be achieved. The critical temperature is given by formula (9) allowing for

$$\varepsilon_F = \varepsilon_{F0}x^{2/3}, \quad p_F = p_{F0}x^{1/3},$$

where ε_{F0} , p_{F0} are the Fermi energy and Fermi momentum of pure ${}^3\text{He}$. According to estimates made in [12], we have

$$\max T_{c0} = T_{c0}(1\%) \approx 10^{-4}\text{K}.$$

The authors of [13] predict an even lower critical temperature:

$$\max T_{c0} = T_{c0}(2\%) \approx 4 \cdot 10^{-6} - 10^{-5}\text{K}.$$

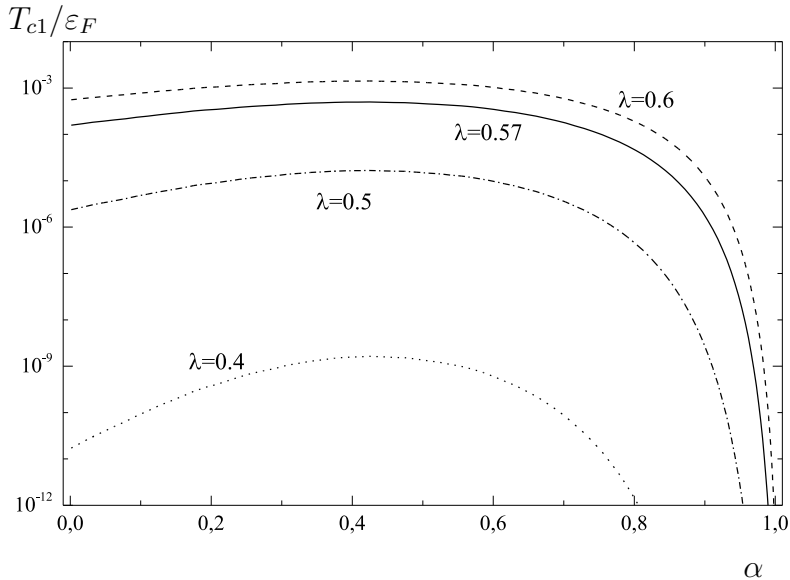


Figure 11: Dependence of T_{c1}/ϵ_F on the degree of polarization α for various λ .

Note that the value $T_{c0} \approx 10^{-5}$ was extracted from spin-diffusion experiments in [13] as a fitting parameter to describe magnetostriction experiments and $T_{c0} \approx 4 \cdot 10^{-6}$ K was obtained in spin diffusion experiments. It should be noted that for a given concentration x the gas parameter of the theory $ap_{F0}x^{1/3}$ depends weakly on pressure. Hence the pressure cannot be considered as an instrument to obtain optimum parameters for s -wave pairing.

For high concentrations ($x > x_0$) the scattering length changes sign $a > 0$ and s -wave pairing becomes impossible. Nevertheless, in this case the subsystem of ^3He atoms may become superfluid, but now with respect to p -wave pairing. The critical temperature is given by formula (32) with λ replaced by $\lambda x^{1/3}$ and ϵ_F replaced by $\epsilon_F x^{2/3}$. It has a maximum at $P = 10$ atm when the maximum ^3He concentration of 9.5% is achieved. Figure 12 gives the dependence of T_{c1} on the concentration calculated by using the extrapolation formula (32). At maximum concentration $x = 9.5\%$ the temperature T_{c1} is of the order of 10^{-5} . A further increase in T_{c1} in solution may occur in strong magnetic field. For example, at $x = 9.5\%$ the maximum of T_{c1} in a field is more than six times that in the absence of a field, leading us to experimentally measurable temperatures of $6 \cdot 10^{-5}$.

Recently the properties of trapped Bose-condensed gases of alkali elements (^{23}Na , ^7Li , ^{87}Rb) have been studied intensively. A combination of laser and evaporative cooling in magnetic traps can reach gas-phase densities of the order of $10^{12} - 10^{14} \text{ cm}^{-3}$ and temperatures of the order of $10^{-6} - 10^{-8}$. In addition these elements may have an anomalously large scattering length a of quasi-resonant origin. For Rb and Na the scattering lengths are positive. It is also found that the scattering length may cover a broad spectrum of values from negative to positive as a result of the Feshbach effect. This effect was observed for ^{23}Na [14].

A logical continuation of studies of Bose condensation in trapped gases of alkali atoms

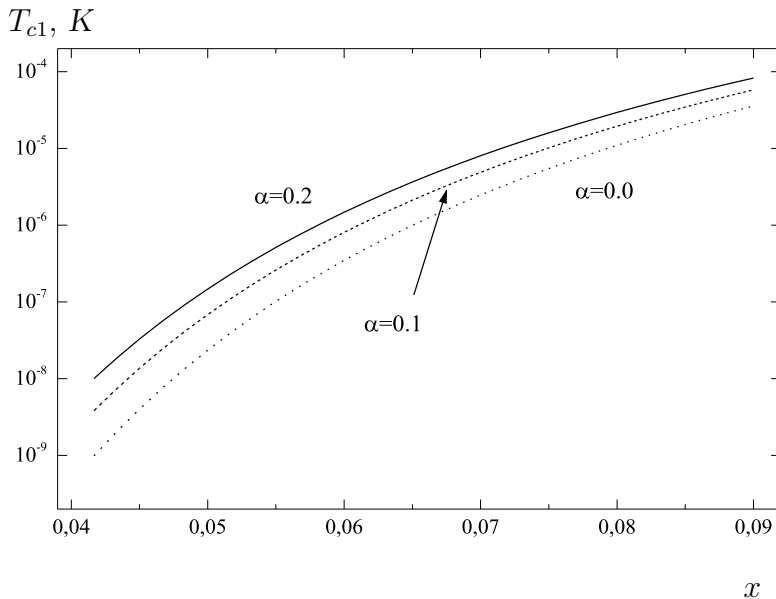


Figure 12: Dependence of T_{c1} on the concentration x in a ${}^3\text{He}$ - ${}^4\text{He}$ mixture for various degrees of polarization: $\alpha = 0.2$ – solid curve, $\alpha = 0.1$ – dashed curve, and $\alpha = 0.0$ – dotted curve.

would be to obtain superfluidity in low density fermionic system in restricted geometry. The case of a negative scattering length makes it possible to achieve s -wave pairing with a transition temperature determined by formula (9). For ${}^6\text{Li}$, for example, we have $a = -2.3 \cdot 10^{-3} \text{Å} < 0$. Thus, for $n \sim 10^{14} \text{cm}^{-3}$ the critical temperature T_{c0} is of the order of $\sim 10^{-6} \text{K}$. Note that because of the Pauli principle the wave function of an s -wave Cooper pair should be antisymmetric with respect to the interchange of quantum numbers characterizing the internal state of the atoms forming the pair. These numbers are indices determining the multiplet component of the hyperfine interaction for the case of zero field (optical trap) or weak magnetic field. They can also correspond to the projections of the nuclear spin when the strong external magnetic field of the trap destroys the hyperfine coupling. Thus, s -wave pairing can only take place between atoms of different gas components. This imposes a very stringent constraint on the closeness of their densities. From the experimental point of view we should have: $|n_1 - n_2| / (n_1 + n_2) \leq T_{c0} / \varepsilon_F \ll 1$. In the opposite case the Cooper pair would have a velocity higher than the critical velocity $v_c \sim T_{c0} / p_F$, and hence will be destroyed. From the experimental point of view, it may therefore prove difficult to achieve this type of pairing experimentally. For p -wave pairing, a Cooper pair may be formed by atoms of the same component (an analog of the A_2 phase in superfluid ${}^3\text{He}$). Note that the superfluid transition temperature in the triplet case may be increased substantially by utilizing the presence of several components in the trap. This increase is similar to the increase in T_{c1} in a magnetic field and is associated with the idea of the separation of channels: Cooper pairing is achieved between particles of one component as a result of the polarization of the other components. In this case, it is possible to obtain a superfluid p -wave pairing temperature of the order of $10^{-7} - 10^{-5}$, which is quite feasible experimentally. By virtue of this fact this type of pairing may be quite promising from the experimental point of view.

In conclusion the authors thank D. Rainer, H.W. Capel, G. Frossati, R. Jochemsen, A.F. Andreev, I.A. Fomin, I.M. Suslov, Yu. Kagan, A.S. Alexandrov, and A.A. Golubov for many useful discussions. This work was supported financially by the Russian Foundation for Basic Research (projects no. 98-02-17077, 97-02-16532, and 96-15-96942) and INTAS (project no. 97-0963).

References

- [1] L.P. Gor'kov and T.K. Melik-Barkhudarov, Zh. Eksp. Teor. Fiz. **40**, 1452 (1961) [Sov. Phys. JETP **13**, 1018 (1961)].
- [2] W. Kohn, J.H. Luttinger, Phys. Rev. Lett. **15**, 524 (1965).
- [3] D. Fay, A. Layzer, Phys. Rev. Lett. **20**, 187 (1968).
- [4] M.Yu. Kagan, A.V. Chubukov, Pis'ma Zh. Eksp. Teor. Fiz. **47**, 525 (1988) [JETP Lett. **47**, 614 (1988)].
- [5] E.M. Lifshitz and L.P. Pitaevskii *Course of Theoretical Physics. Vol. 9. Statistical Physics* (Nauka, Moscow, 1978; Pergamon Press, New York, 1980).
- [6] L.D. Landau and E.M. Lifshitz, *Quantum Mechanics: Non-Relativistic Theory* (Nauka, Moscow, 1989, 4th ed.; Pergamon Press, Oxford, 1977, 3rd ed.).
- [7] A.A. Abrikosov, L.P. Gor'kov, and I.E. Dzyaloshinskii, *Methods of Quantum Field Theory in Statistical Physics* (Nauka, Moscow, 1962; Prentice-Hall, Englewood Cliffs, 1963).
- [8] *Problems of High-Temperature Superconductivity*, Ed. by V.L. Ginzburg and D.A. Kirzhnits (Nauka, Moscow, 1977).
- [9] A.S. Alexandrov, A.A. Golubov, Phys. Rev B **45**, 4769 (1992).
- [10] M.Yu. Kagan and A.V. Chubukov, Pis'ma Zh. Eksp. Teor. Fiz. **50**, 483 (1989) [JETP Lett. **50**, 517 (1989)].
- [11] G.-H. Oh, Y. Ishimoto, T. Kawae, M. Nagasiva, O. Ishikawa, H. Hata, T. Kodama, and S. Ikekata, JLTP **95**, 525 (1994).
- [12] E. Østgaard, E.P. Bashkin, Physica B **178**, 134 (1992).
- [13] P.G. van der Haar, G. Frossati, and K.S. Bedell, JLTP **77**, 35 (1989).
- [14] J. Stenger, S. Inouye, M.R. Andrews, H.-J. Miesner, D.M. Stamper-Kuru, and W. Ketterle, Phys. Rev. Lett. **82**, 2422 (1999).
- [15] M.A. Baranov, M.Yu. Kagan, and Yu. Kagan, Pis'ma Zh. Eksp. Teor. Fiz. **64**, 301 (1996) [JETP Lett. **64**, (1996)].